MINERALOGICAL AND GEOLOGICAL DIVERSITY OF VAVILOV CRATER DERIVED USING REMOTE SENSING DATA. D. D. Patel[1], S. M. Patel[1], P.M. Solanki[1]. [1]M. G. Science Institute, India (email: deepp213@gmail.com).

Introduction: Vavilov (0.8 S° 137.9 W°) is a prominent lunar impact crater with the average diameter of 99 km located on the far side of the moon [1]. It lies to the west of the walled plain Hertzsprung, southwest to the relatively smaller crater Chaucer, and north-east to Sechenov crater. The model age of Vavilov crater is 1.7 ± 0.1Ga and being of Copernican age [2] It is a complex crater with a prominent central peak, a roughly circular rim, flat hummocky crater floor, and a number of wall terraces. Floor fractures and cooling cracks are also noticeable on the floor of the crater.

Data Acquisition: The Moon Mineralogy Mapper (M3) is a NASA-supported guest instrument on ISRO's Chandrayaan-1 lunar remote sensing mission. The M^3 is a pushbroom spectrometer that works in the visible to near-infrared (0.42-3.0µm) ranges, where highly diagnostic mineral absorption bands can be found at 140 m/pixel spatial resolution with 86 spectral channels [3]. M^3 images were downloaded from the PDS (Planetary Data System) Geoscience Node where the data is in the public domain.

The morphological analysis is carried out by using the Wide Angle Camera (WAC) and Narrow Angle Camera (NAC) images, onboard Lunar Reconnaissance Orbiter (LRO) of NASA. The calibrated NAC images were downloaded from PILOT (Planetary Image Locate Tool) which is a web-based search tool for the Unified Planetary Coordinate (UPC) database of the PDS developed by the USGS Astrogeology Science Centre and the NASA PDS Imaging Node.

Methodology: Minerals are identified from the study of their spectral profiles in normal as well as continuum removed reflectance. Continuum removal is applied to aid the characterization of the 1µ- and 2µ-bands for identifying the minerals [3]. The georeferencing, mosaicking and spectral sample collection was performed in the Environment for Image Processing (ENVI) software.

Similar mapping of the features was done by having evident geological boundaries based on their physical properties including relative elevation, structural complexities, albedo, and surface texture [4]. All these features are analyzed and mapped using LROC NAC images along with their morphometrical studies which are carried out with the elevation graphs in ArcGIS software.

Results and discussion: The compositional analysis is carried out by the spectral graphs as each mineral has its unique absorption bands. From the understanding of the minerals present, their origin, and the clues about the geological evolution of the moon can be speculated [5]. From the compositional analysis, minerals like Low-Calcium Pyroxene (LCP), High-Calcium Pyroxene (HCP), plagioclase, and mixtures of pyroxene-plagioclase, olivine-pyroxene are detected from various parts of the crater. Diversity in the composition can be related to the presence of several morphological features.

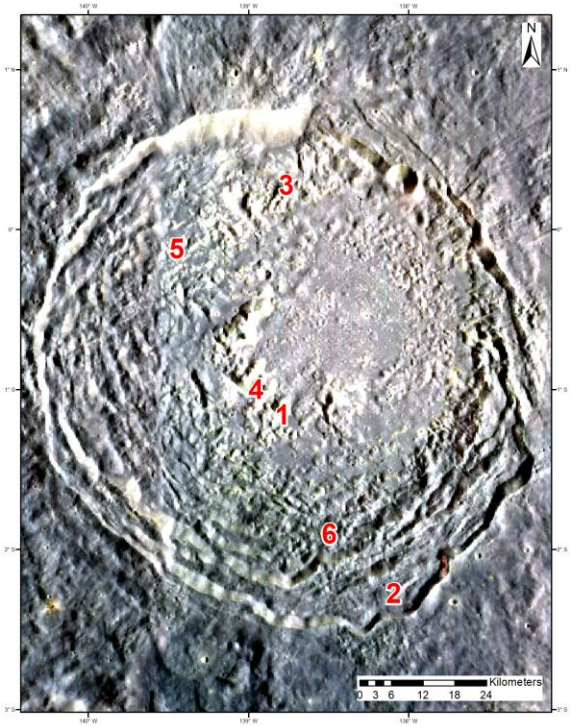

Figure 1: M^3 FCC (R: 930 nm, G: 1249 nm and B: 2018 nm) showing reflectance spectra locations 1-Plagioclase, 2-Mg Spinel, 3-HCP, 4-Plagioclase+Pyroxene, 5-Olivine+Pyroxene, 6-LCP

At the central peak at location-1, plagioclase shows strong absorption at 1250µm indicating the presence of FeO, which indicates upper crustal composition. This is due to the location of the crater in the highland area. The presence of Mg-spinel mineral at location-2, suggesting deep-seated lithological exposure [6]. HCP is observed at location-3, The HCP has a lower crustal origin, i.e., at lesser depths than that of LCP [7]. Mixture of plagioclase and pyroxene is also present in the central peak at location-4. Olivine and pyroxene mixtures are present in location-6 and in small areas indicating their secondary origin by melt recrystallisation

or can be of exogenetic nature [8]. The presence of LCP at location-6 that the deeper material has been exposed here in comparison to the surrounding area.

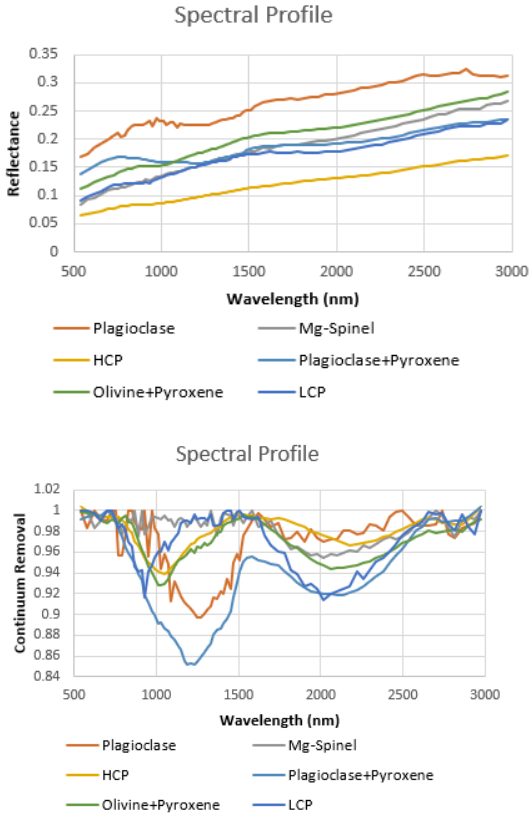

The rim of the crater is roughly circular, slightly bulging outwards towards the south-east. The elevation of the rim is not even, north-eastern part being relatively lower in elevation than the surrounding crater. The central mound is asymmetrical, crescent shaped, off-centered, positioned slightly towards the west. It trends roughly north to south. A relatively high isolated mount is present in the southern part of the crater. he inner walls of the rim display several terraces, particularly to the southeast. Sometimes along the inner crater wall step-like, curvy slump features are found which are known as terraces. Secondary craters are formed as a result of the impact of clustered ejecta material which flown out during the primary impact [10].

The floor is on the north-east, with a number of isolated mounds with relatively higher albedo. The floor consists of a number of floor fractures and impact flows. Cooling cracks are also prominent. Slumping is very extensive in the northern, north-west, and southern part of the crater, which might have occurred due to gravity induced mass movement [11]. Boulder fields are seen at the base of the flank and along the concentric floor-fractures around the central peak, they are also extensive on wall terraces. Boulder tracks correspond to rock falls that were a consequence of erosion via impact or seismic activity in the region [12]. The crater is overlapped by another younger crater in the north-eastern rim.

A morphological map of all the features discussed have been prepared by keeping LROC-WAC and NAC images as a base in ArcGIS software on a scale of 1:25,000.

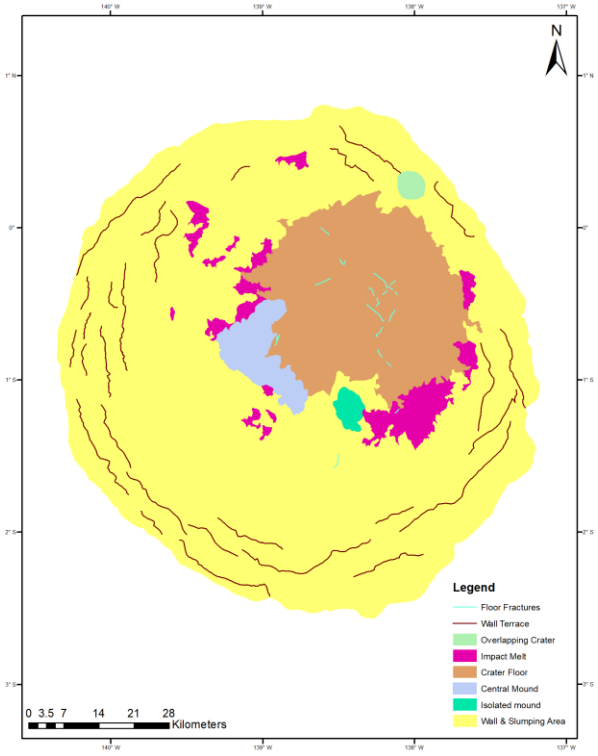

Figure 2: Morphological Map of Vavilov crater produced using high resolution NAC and WAC images in ArcGIS software.

Acknowledgements: We wish to acknowledge M^3 (Level-2 data) and LROC team for providing high resolution data in the public domain and supplying the data through PDS Geoscience Node.

References: [1] Andersson L. E. and Whitaker, E. A., (1982) *NASA Catalogue of Lunar Nomenclature*, *1097*, 147. [2] Kirchoff, M. R., et al., (2013) *Icarus*, *225*(1), 325-341. [3] Pieters C M, et al. (2009) *Curr. Sci. 96(4)* 1–6 [4] Thaker A. D., et al 2020 *Planet. Space Sci.*, *184*, 104856 [5] Burns, R. G. 1970, *Amer. Mineral*, *55*, 1608–1632. [6] Pieters, C. M., et al. (2014), *Amer. Mineral*, 99(10), 1893-1910. [7] Martinot, M., et al. (2018), *JGR: Planets*, *123(2)*, 612-629. [8] Brearley, A. J., et al. (1998), *Planetary materials*, C1. [9] Mittlefehldt, D. W., et al. (2018). *Planetary materials*, 523-718. [10] Hargitai, H., 2015, *Encyclopedia of Planetary Landforms*, *Springer*, *New York*, 1884. [11] Greeley, R., Klemaszewski, et al. (2000) *Planet. and Space Sci*., *48*, 829-853. [12] Kumar P. S. et al. (2016) *JGR Planets*, *121*, 147–179